

PACS numbers: 42.55.Px; 42.60.Lh
DOI: 10.1070/QE2008v038n07ABEH013824

Semiconductor optical amplifiers for the 1000 – 1100-nm spectral range

A.A. Lobintsov, M.V. Shramenko, S.D. Yakubovich

***Abstract*. Two types of semiconductor optical amplifiers (SOAs) based on a double-layer quantum-well (InGa)As/(GaAl)As/GaAs heterostructure are investigated. The optical gain of more than 30dB and saturation output power of more than 30 mW are achived at 1060 nm in pigtailed SOA modules. These SOAs used as active elements of a tunable laser provide rapid continuous tuning within 85 nm and 45 nm at output powers of 0.5 mW and more than 30 mW, respectively.**

Keywords: *semiconductor optical amplifier, quantum-well heterostructure, tunable laser.*

1. Introduction

Investigations of semiconductor optical amplifiers (SOAs) began soon after the advent of semiconductor lasers [1, 2]. To realise SOAs, various methods for suppression of a positive optical feedback in laser diodes were elaborated. Presently the designs with a narrow (straight or bent) waveguide active channel with the axis tilted to AR-coated crystal facets are generally used. Semiconductor optical amplifiers operating in the amplified spontaneous emission (ASE) regime have evolved into the separate class of semiconductor emitters, which are called superluminescent diodes (SLDs) [3].

Semiconductor optical amplifiers operating in the telecommunication spectral range (1300 – 1650 nm) have found wide applications as amplifiers, modulators and switchers of optical signals in various components of fibreoptic data transmission systems. COVEGA, InPhenix, DensLight and some other companies manufacture a commercially available range of products of this type. As for short-wavelength (near IR) SOAs, they are rather used as active elements in single-frequency and tunable external cavity lasers containing spectrally selective components [4 – 6].

In the last decade, the method of optical coherence tomography (OCT) for *in vivo* imaging of biological tissues with micron spatial resolution is being rapidly developing [7]. Either broadband (low coherent) cw light sources (mostly SLDs) or rapidly tunable lasers are used in OCT systems. The widest application of OCT systems have found in ophthalmic diagnostics [8, 9], where near-IR range (800 – 900 nm) light sources are used due to a minimum optical absorption in aqueous humor in this spectral range and interferometric signals are recorded with high-speed spectrometers equipped with CCD arrays. In 2006 several companies (Optopol Technology, Topcon Medical Systems, OPTOVUE and others) have started a serial production of diagnostic equipment of this type.

Light sources emitting in the spectral range from 1000 to 1100 nm have attracted increasing interest for ophthalmic diagnostics in the last years. This emission penetrates deeper into the eyeground and provides (e.g. [10]) more detailed information on some eye pathologies. The second transparency window of the aqueous humor is located in the region from 1040 to 1060 nm. And although optical absorption in it is noticeably higher than that in the near-IR range, this disadvantage can be compensated by higher exposures because the admissible eye-safe irradiation doses in this spectral region are considerably higher. Unfortunately efficient CCD arrays for this spectral band are still not commercially available and it is necessary to use a conventional photodetector together with a tunable laser. Such lasers can be based on Yb^{+}-doped optical fibres [11]. However, tunable lasers based on SOAs are preferable due to their higher efficiency. According to the estimates of researchers at Micron Optics, the manufacturer of lasers with original Fabry – Perot tunable fibre filters (FPTFFs), to develop a laser required for OCT, it is necessary to have a SOA module for the 1040 – 1060-nm range with the output power saturation level no less than 30 mW. To our knowledge, currently only a single SOA version is presented at the optoelectronic market for this spectral band, namely QSOA-1050 by QPHOTONICS with the optical gain up to 20 dB and output power saturation at 10 mW. Thus, the development of highly efficient SOAs is of current interest, and our paper is devoted to this problem.

2. Experimental samples

Investigated SOA samples were fabricated from the (InGa)As/(GaAl)As/GaAs double-quantum-well (DQW) heterostructure grown by MOCVD epitaxy [12]. The design of the double-pass SOA of type I is described in detail in [5]. Its single-mode active channel of length 600 μm was J-shaped. The active channel axis was tilted by 7° with respect

A.A. Lobintsov, M.V. Shramenko Superlum Diodes Ltd., P.B. 70, 117454 Moscow, Russia; e-mail: shramenko@superlumdiodes.com;
S.D. Yakubovich Moscow State Institute of Radio-Engineering, Electronics and Automation (Technical University), pr. Vernadskogo 78, 117454 Moscow, Russia; e-mail: yakubovich@superlumdiodes.com

Received 14 February 2008
Kvantovaya Elektronika **38** (7) 661 – 664 (2008)
Translated by D.S. Mamedov

to the normal to the output crystal facet and was orthogonal to the rear facet. The output facet was AR coated providing the residual effective reflectance smaller than 10^{-4}, while the rear crystal facet had a reflection coating (RC) with the reflectance 3 %. A SOA of type II had the design traditional for single-pass amplifiers. Its straight active channel of length 1600 μm was tilted by 7° with respect to both AR-coated crystal facets (see insets in Fig. 1). Samples were assembled in Butterfly housings with thermoelectric microcoolers and thermistors providing thermal stabilisation in the operation regimes. Polarisation-preserving Corning PANDA fibres were used as input/output pigtails. Modules of types I and II had one or two fibre pigtails, respectively. The slow axis of the fibre was oriented parallel to diode heterolayers.

In the absence of optical feedback (for skewed output ends of the fibre) SOA modules have the properties of SLDs. The depth of the residual modulation of the spectrum by Fabry–Perot modes did not exceed 5 % and 2 % for modules of types I and II, respectively. The SOA modules with fibres having end facets cleaved normally to the fibre axis operate as lasers with an external nonselective fibre cavity. Typical power and spectral characteristics of experimental samples in superluminescent and lasing regimes are shown in Fig. 1.

3. Experimental results

The SOA of type I with moderate power characteristics played an auxiliary function in our study and was used to assemble the laboratory prototype of the external fibre cavity semiconductor laser with the acousto-optic tunable filter (AOTF). This laser was employed to study the transfer characteristics of the highly efficient SOA of type II. A similar laser emitting in the 820–870-nm spectral range and described in detail in [5] differed from this prototype only by the active element: the SOA-371 module was replaced by the SOA of type I. The optical scheme of the laser is shown in Fig. 2a. Acousto-optical tunable filter (*2*) and fibreoptic collimators (*3*) in this scheme had AR coatings for the 820–870-nm spectral range but introduced high optical losses in the 1000–1100-nm range. Nevertheless, the achieved output power of ~1.0 mW and the tuning range exceeding 80 nm were sufficient for measuring the optical gain spectra and transfer characteristics of the SOA of type II up to the output power saturation. Figure 3 shows the change in the injection current of the SOA of type I during laser tuning, which was performed by means of the electronic system for automatic output power control (APC). AOTF controller (*8*) allowed both manual wavelength tuning and linear sweeping in the specified spectral region with a frequency of up to 200 Hz. The instant linewidth of the laser did not exceed 0.05 nm.

The output laser radiation was incident to the input of a measuring circuit (Fig. 2b). Input optical isolator (*9*) (AC Photonics PMIS10) prevented parasitic optical feedback caused by reflections of emission of SOA (*11*) from laser mirror (*4*). Variable optical attenuator (*10*) (OZ Optics BB-500) was used to change the input signal power in a wide range. The power was accurately measured with fibreoptic Y-coupler (*5*) (OZ Optics FOBS-12P) calibrated in the required spectral range. The input and output signals were measured with calibrated Newport 1830-C power meters (*12*) upon thermal stabilisation of both SOAs at 25 °C which was provided by PILOT-4 controller (*7*).

Small-signal optical gain spectra of the SOA of type II at various pump levels are shown in Fig. 4a. As the SOA injection current is increased, the gain band broadens to the short wavelength region. This is explained by the involvement of not only stimulated quantum transitions from the fundamental subband but also from the first excited subband to optical amplification [12]. The fibre-to-fibre optical gain for $I_{SOA} = 210$ mA at 1060 nm was 32 dB. The gain band at the −3 dB level was more that 30 nm and at the −10 dB level – more than 55 nm. This is the record result for SOAs in this spectral range. The transmission characteristics

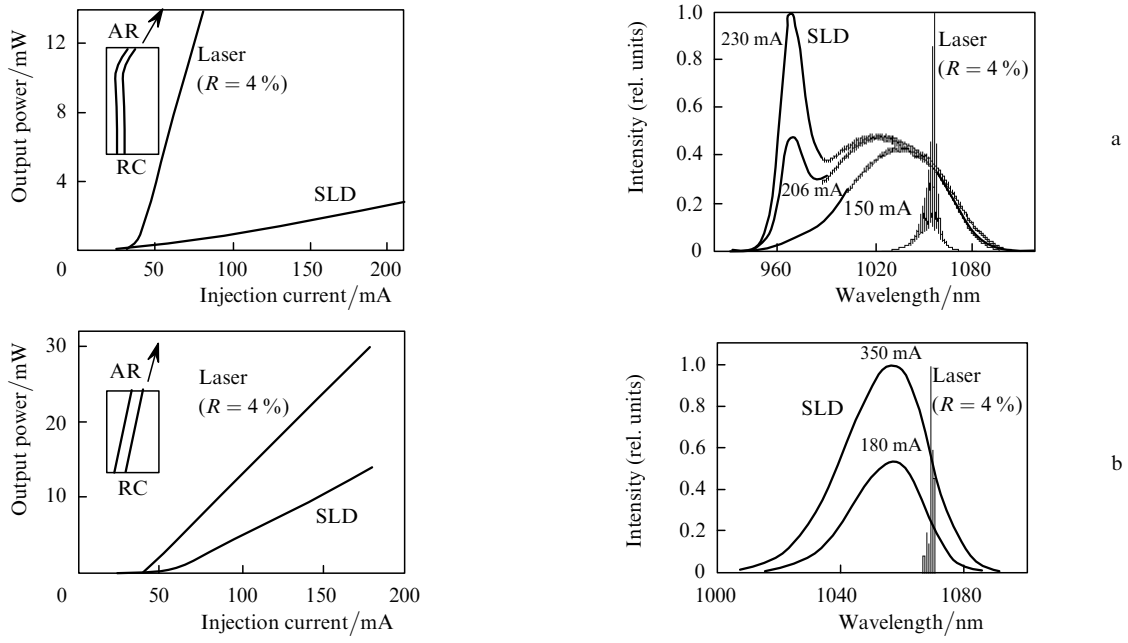

Figure 1. Light–current characteristics and emission spectra of SOA modules of type I (a) and type II (b) in lasing and superluminescence regimes.

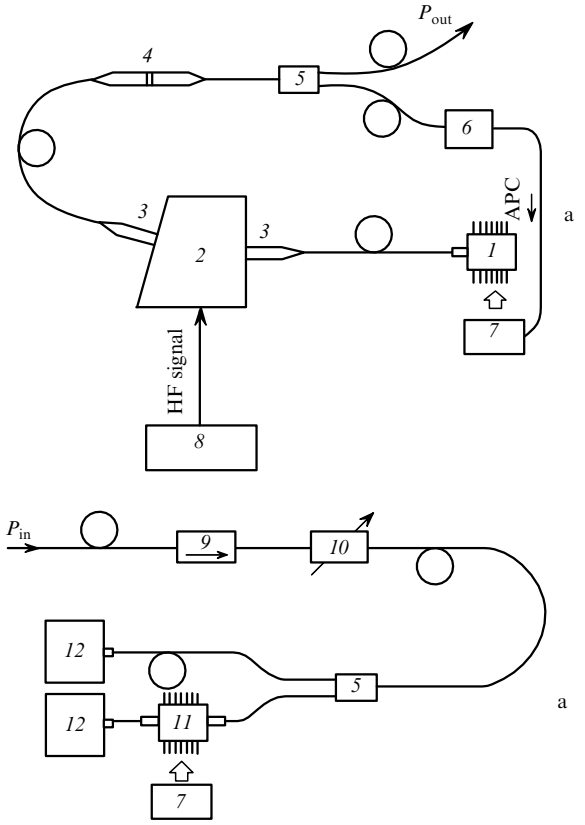

Figure 2. Optical scheme of the tunable semiconductor laser based on the SOA of type I with AOTF in an external fibre cavity (a) and scheme for measuring the transmission characteristics of the SOA of type II (b): (*1*) SOA module of type I; (*2*) AOTF; (*3*) fibreoptic collimator; (*4*) fibre mirror ($R = 30$ %); (*5*) fibreoptic Y-coupler (96 : 4); (*6*) photodetector of the APC loop; (*7*) SOA controller; (*8*) AOTF controller; (*9*) optical isolator; (*10*) variable optical attenuator; (*11*) SOA module of type II; (*12*) optical power meter.

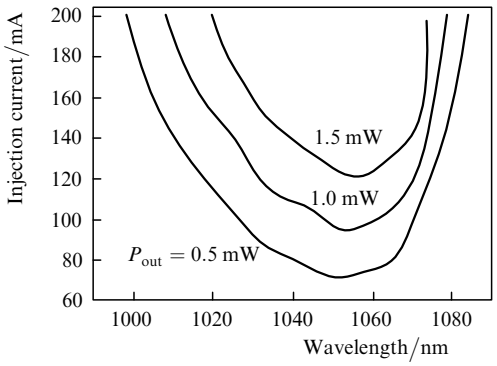

Figure 3. Change in the injection current of the SOA of type I upon laser tuning at constant output powers.

of the SOA of type II at a wavelength of 1060 nm are presented in Fig. 4b. The optical gain was calculated from the expression:

$$G = [P_{out} - P_{out}(P_{in} = 0)]/P_{in}. \quad (1)$$

The gain saturation level (the decrease in the gain G by 3 dB) strongly depends on the pump level and for $I_{SOA} = 151$ mA it was ~ -20 dBm (10 μW). To avoid a catastrophic SOA degradation, we limited the output power to 16 dBm (40 mW). SOA lifetime testing was not performed. Note,

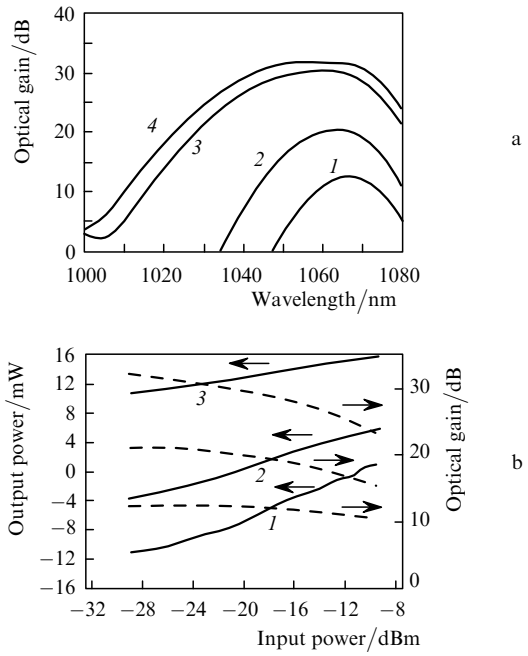

Figure 4. Small signal gain spectra (a) and transmission characteristics of the input signal at 1060 nm (b) obtained for the SOA of type II for injection currents 36 (*1*), 50 (*2*), 151 (*3*), and 210 mA (*4*).

however, that SLD-531-HP modules fabricated from the same heterostructure are highly reliable at fibre output powers up to 30 mW. As mentioned in the introduction, this value satisfies the requirements for light sources for ophthalmic OCT applications in this spectral range.

The laboratory prototype of such a light source was realised by excluding from the described optical scheme (see Fig. 2) optical attenuator (*10*) and coupler (*5*). SOA (*11*) played the function of the output power amplifier. Although a swept frequency of 200 Hz is not sufficient for OCT applications, this prototype allowed us to estimate top achievable levels of power and spectral characteristics. Figure 5 shows the output emission spectra for the constant injection current $I_{SOA} = 151$ mA and different wavelengths of the master laser. In the range of a maximum gain almost a complete suppression of superluminescence is observed, and the spectral brightness of the useful signal exceeds the background level by more than four orders of magnitude. The integrated power of the superluminescent 'pedestal' is comparable with the useful signal power. Figure 6 demonstrates the dependences of the output power and the output emission spectrum on the input signal wavelength. One can see, in particular, that the output power in the 1030 – 1070-nm spectral band exceeds 30 mW, while the spectral brightness of the useful signal exceeds the background level by more than 30 dB.

In principle this prototype can be significantly improved. The use of an APC (automatic power control) loop circuit tracing the injection current of the output SOA would provide a constant level of the output power over the entire tuning range. The use of the AOTF at the scheme output, which is identical to the AOTF of the master laser and is tuned synchronously with the latter would provide the increase in SMS approximately by two orders of magnitude. Finally, the use of higher speed AOTFs would allow increasing the sweep frequency. All these improvements are the subject of further research and developments.

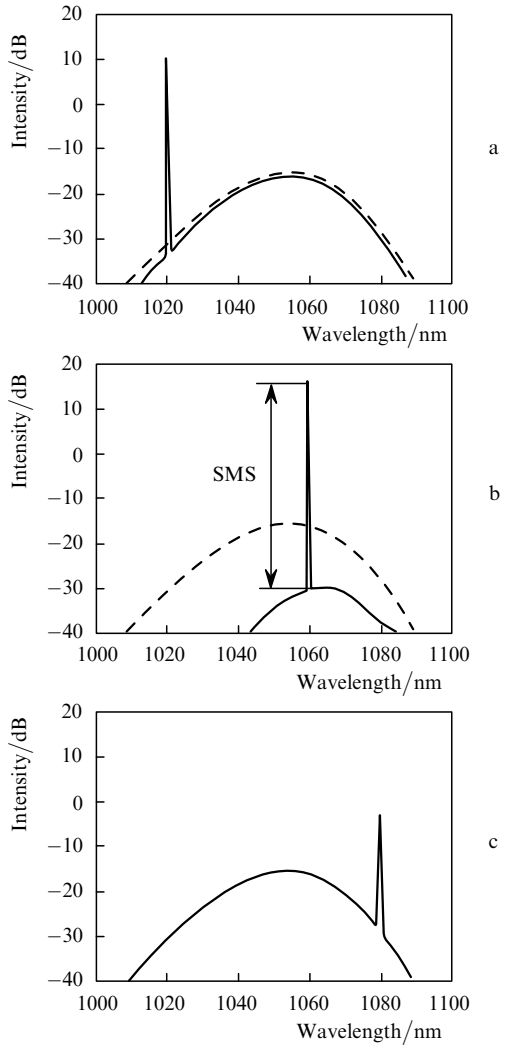

Figure 5. Output emission spectra of the SOA of type II in the absence (dashed curve) and presence of the 0.5-mW input signal at wavelengths 1020 (a), 1060 (b), and 1080 nm (c).

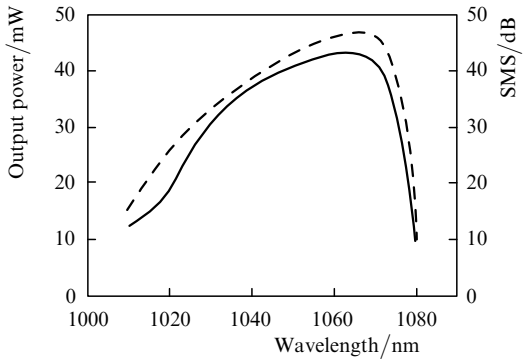

Figure 6. Dependences of the output power (solid curve) and the excess of the spectral brightness of the output signal over the superluminescence background level (dashed curve) on the 0.5-mW input signal wavelength for SOAs of type II.

4. Conclusions

Highly efficient SOA modules with the maximum optical gain exceeding 30 dB at 1060 nm, the gain bandwidth more than 30 nm, and the output power saturation level above 30 mW have been developed. As far as we know, such a combination of SOA working characteristics has been achieved for the first time. The outlook for using these modules as active elements in external fibre cavity tunable lasers has been demonstrated.

Acknowledgements. The authors thank A.A. Marmalyuk for growing highly efficient DQW structures, L.N. Magdich for the development of unique AOTFs, and A.T. Semenov for his attention to this research. The work was partially supported by the Ministry of Education and Science of the Russian Federation (Project RPN 2.1.1.1094).

References

1. Growe J.W., Ahearn W.E. *IEEE J. Quantum Electron.*, **2** (8), 283 (1966).
2. Kosonocky W.F., Cornely R.H. *IEEE J. Quantum Electron.*, **4** (4), 125 (1968).
3. Alphonse G.A. *Proc. SPIE Int. Soc. Opt. Eng.*, **4648**, 125 (2002).
4. Lim H., de Boer J.F., Park B.H., Lee E.C.V., Yelin R., Yun S.H. *Opt. Express*, **14** (13), 5937 (2006).
5. Andreeva E.V., Magdich L.N., Mamedov D.S., Ruenkov A.A., Shramenko M.V., Yakubovich S.D. *Kvantovaya Elektron.*, **36**, 324 (2006) [*Quantum Electron.*, **36**, 324 (2006)].
6. Shrinivasan V.J., Huber R., Gorczynska I., Fujimoto J.G., Jiang J.Y., Reisen P. *Opt. Lett.*, **32** (4), 361 (2007).
7. Fersher A.F., Drexler W., Hitzenberger C.K., Lasser T. *Rep. Prog. Phys.*, **66**, 239 (2003).
8. Drexler W., Morgner U., Ghanta R.K., Kartner F.X., Schuman J.S., Fujimoto J.G. *Nature Medicine*, **7** (4), 10 (2001).
9. Royce W.S., Chen B.A., Jay S., Duker M.D., Shrinivasan F., Fujimoto J.G. *Rev. Ophtalmol.*, July, 84 (2007).
10. Povazay B., Bizheva K., Hermann B., Unterhuber A., Sattmann H., Ferscher A.F., Drexler W., Schubert C., Ahnelt P.K., Mei M., Holzwarth R., Wadsworth W.J., Knight J.S., Russel P.S.J. *Opt. Express*, **11** (17), 1980 (2003).
11. Nielsen F.D., Thrane L., Black J., Hsu K., Bjarklev A., Anderesen P.E. *Proc. SPIE Int. Soc. Opt. Eng.*, **5861**, 5851OH-1 (2005).
12. Lapin P.I., Mamedov D.S., Marmalyuk A.A., Padalitsa A.A., Yakubovich S.D. *Kvantovaya Elektron.*, **36**, 315 (2006) [*Quantum Electron.*, **36**, 315 (2006)].